Structure and Propagation of a Modeled MJO – Emphasis on the East Pacific

David J. Raymond

Physics Department and Geophysical Research Center
New Mexico Tech
Socorro, NM 87801, USA

1 Introduction

Raymond (2001) presented an intermediate numerical model of the Madden-Julian oscillation (MJO) (Madden and Julian, 1994) which reproduced many aspects of the structure and propagation of the observed disturbance in the western Pacific. Recent observational work has shown the importance of the MJO to deep convection and tropical cyclogenesis in the eastern Pacific region (Maloney and Hartmann, 2000, 2001a,b; Molinari and Vollaro, 2000). The recently completed EPIC2001 (East Pacific Investigation of Climate, 2001; Raymond et al., 2003a) field program casts light on how the MJO interacts with convection in this region.

In this talk I first present results from EPIC2001 which show how convection is driven over the east Pacific warm pool south of Mexico. I then present a simulation using the model of Raymond (2001) in which the observed convective driving mechanisms are operative. The results suggest that MJO dynamics are central to the functioning of deep convection and the intertropical convergence zone (ITCZ) in the eastern Pacific.

2 EPIC2001 results

Unlike the western Pacific, the far eastern Pacific exhibits a strong, cross-equatorial sea surface temperature (SST) gradient. Waters on and south of the equator are relatively cold most of the year, and generally are covered with low-level stratus or stratocumulus clouds. North of the equator the warmest waters in the boreal summer are immediately adjacent to the Mexican coast, with SSTs high enough to support deep convection occurring north of $5^\circ - 6^\circ$ N.

As figure 1 shows, convection is both highly intermittent and distributed broadly in latitude in this region. The intermittency is most obviously related to the passage of easterly waves, which often amplify into tropical storms as they move to the west through this region. The longitude-time plot shown in figure2 illustrates this westward movement.

Less obvious is the existence of a longer-time-scale modulation of deep convection in this region. Figure3 shows that the four tropical storms which developed in the east Pacific during EPIC2001 occurred together during a period of overall positive westerly wind anomalies at $810 - 830$ hPa. Immediately after the development of tropical storm Lorena (L in figures 2 and 3), the winds at this level switched to strong easterly. Reanalysis products show that this transition coincided with the trailing edge of an eastward-propagating westerly wind anomaly most likely associated with the departure of the active phase of the MJO (Eric Maloney, personal communication). Interestingly, these zonal winds were nearly in geostrophic balance, as the middle panel of figure 3 indicates.

Also evident from figure 3 is the correlation between stronger surface winds, and hence surface heat fluxes, and low infrared brightness temperatures over the warm waters of the east Pacific. This supports the flux-driven

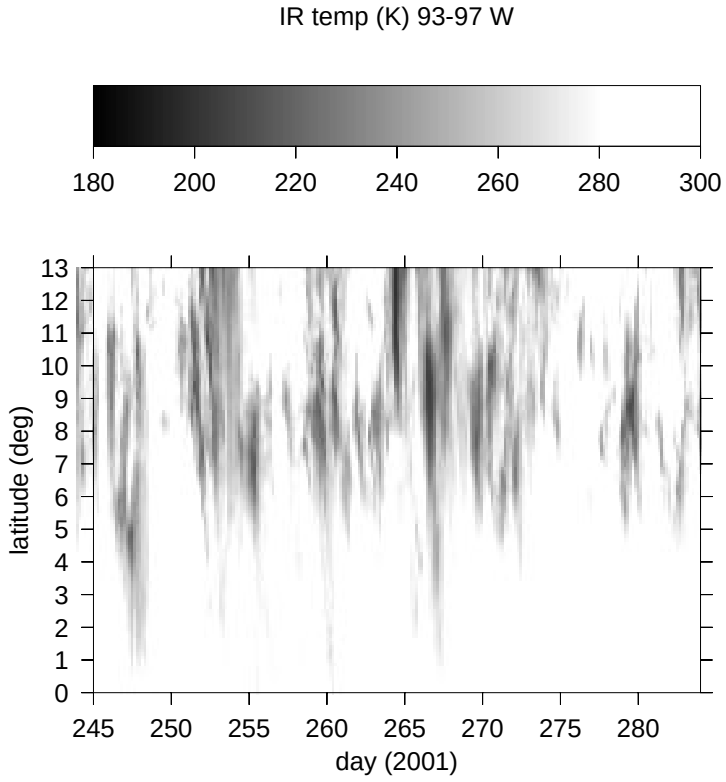

Figure 1: Satellite infrared brightness temperature as a function of latitude and time, averaged over 93° – 97° *W for the period of EPIC2001.*

theory of deep convection propounded by Raymond (1995), Raymond et al. (2003b), and others. Furthermore, the strongest surface winds tend to be southerlies or southwesterlies.

The meridional SST gradient in the east Pacific causes a corresponding gradient in the temperature of the planetary boundary layer (PBL). If no horizontal pressure gradient exists at the top of the PBL, the hydrostatic equation guarantees one at the surface, with lower pressures to the north. This pressure gradient and the Coriolis force are what drive the climatological low-level southwesterly winds in the region. Anything which creates a negative meridional pressure gradient at the PBL top reinforces the gradient derived from the SST gradient, and causes stronger surface southwesterlies which reach further north. Likewise, a positive pressure gradient there tends to oppose the SST-derived gradient, resulting in weaker southwesterlies which terminate further south.

Figures 4 and 5 show two extreme cases. On 23 September 2001 there was a strong negative pressure gradient aloft, strong surface southerly winds extending beyond 10° N, and strong deep convection, as indicated by the low infrared brightness temperatures. On 2 October 2001 the PBL-top pressure gradient was positive, surface southerlies were weaker, and they extended only to about 5° N. Virtually no deep convection was present on this day, as the high infrared brightness temperatures show.

As was shown in figure 3, the zonal winds at the PBL top are in reasonable geostrophic balance with the meridional pressure gradient at that elevation. Thus, the negative pressure gradient at 1600 m in figure4 is accompanied by westerlies at this elevation, whereas the positive pressure gradient is related to the PBL-top easterlies in figure 5. Thus, westerlies aloft appear to be related to stronger southwesterly surface winds and stronger deep convection in the east Pacific, whereas easterlies aloft are related to convectively suppressed conditions. This supports the observations of Maloney and Hartmann (2001; 2002a,b) and Molinari and Vollaro (2001) that westerly winds near 850 hPa are correlated with stronger deep convection and hence tropical cyclogenesis, and it provides a mechanism to explain this result.

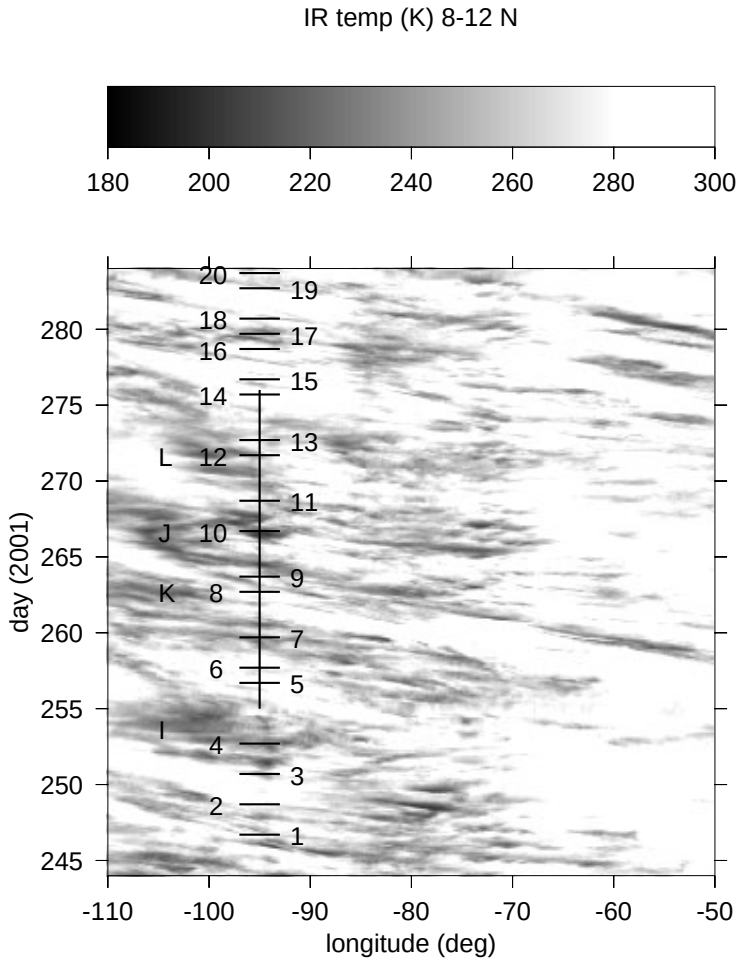

Figure 2: Satellite infrared brightness temperature as a function of longitude and time over the period of EPIC2001, averaged over $8^\circ - 12^\circ$ *N. The vertical line indicates the presence of the ship* Ron Brown *at* 95° *W,* 10° *N and the horizontal lines indicate aircraft missions flown during the project. The letters indicate the passage of tropical storm precursors.*

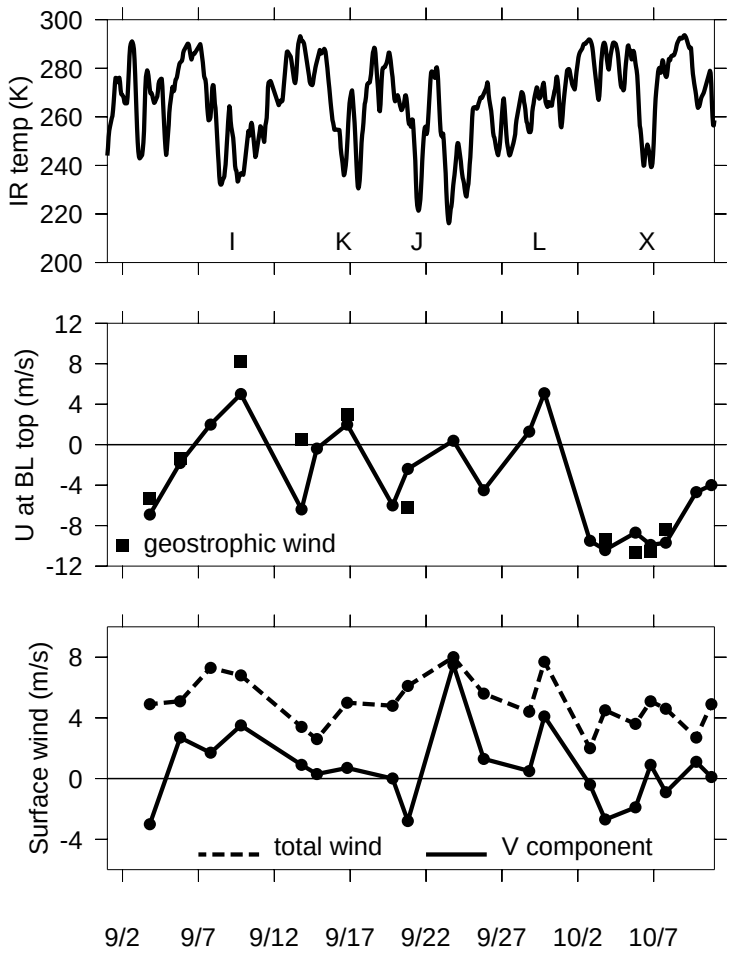

Figure 3: Time series for EPIC. The top panel shows the GOES infrared brightness temperature averaged over the ITCZ study region. The letters I, J, K, and L indicate the passage of tropical storm precursors by 95° *W. The letter X indicates convection apparently associated with a strong easterly jet. The middle panel shows the average zonal wind between* 810 *and* 830 *hPa from dropsondes in the ITCZ study region, defined as the box bounded by* $93^\circ - 97^\circ$ *W and* $8^\circ - 12^\circ$ *N. The box symbols show the geostrophic zonal wind near* 810 *hPa from P-3 aircraft in situ pressure measurements. The bottom panel shows the meridional and total wind averaged over the ITCZ study region near the surface. Dropsonde winds were averaged over* $980 - 1000$ *hPa to obtain these results.*

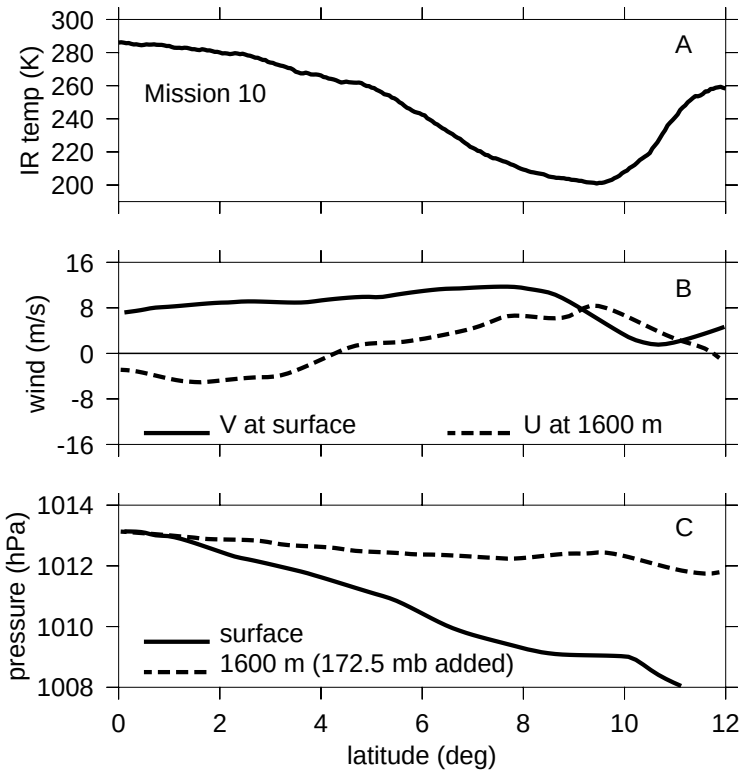

Figure 4: Conditions as a function of latitude along 95° *W on 23 September 2001. (a) Infrared brightness temperature; (b) meridional surface wind and zonal wind at* 1600 *m; (c) pressure at the surface and at* 1600 *m.*

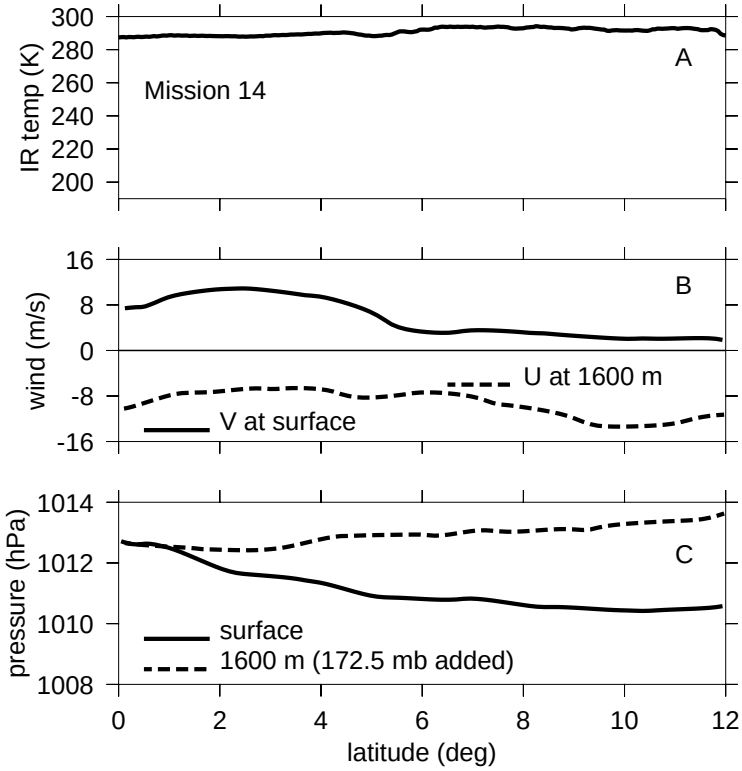

Figure 5: As in figure 4 except for 2 October 2001.

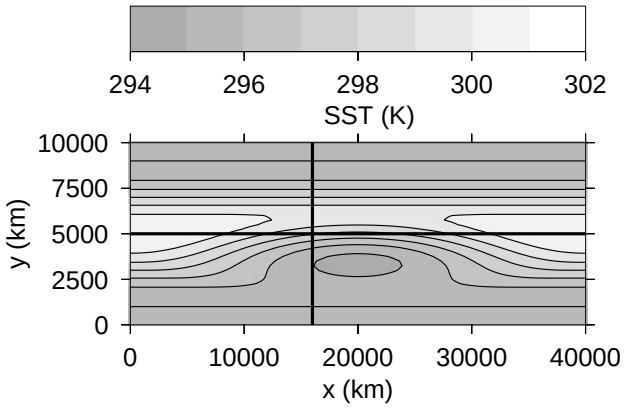

Figure 6: SST distribution for three-dimensional simulation. The horizontal line is the equator and the vertical line designates the longitude of the "east Pacific" section presented in this talk.

3 MJO simulation

I now compare two simulations using the model of Raymond (2001). The first is a three-dimensional simulation on an equatorial beta plane with a computational domain of 40000×10000 km. Boundary conditions are periodic in the east-west direction, with rigid walls at $y = 0, 10000$ km. The SST distribution is illustrated in figure 6 and is intended only to be a rough approximation of the actual situation on the earth, where the western Pacific has a broad, cross-equatorial SST maximum, while the eastern Pacific and Atlantic have narrow SST maxima north of the equator. Other details of the simulation are the same as in Raymond (2001).

Figure 7 shows the zonal wind averaged over the elevation range $1-2$ km in a longitudinal strip 1000 km north of the equator, or directly over the warmest water at longitude $x = 20000$ km. MJO-like disturbances originate over the western part of the warm pool at approximate intervals of 4500 ks (52 d), propagate to the east at about 5 m s^{-1}, and decay over the narrow band of warm water north of the equator. This is not unlike the actual behavior of the MJO.

Figures 8, 9, and 10 show the low level wind structure and rainfall rate for the growing, mature, and decaying phases of the MJO. The structure of the mature disturbance is generally the same as described by Raymond (2001) – latent and sensible heat fluxes produced by a near-equatorial westerly jet feed convection, which maximizes at the eastern exit region of the jet.

Of primary interest here is the structure of the decaying disturbance, as illustrated in figure 10. Due to the cold water on the equator, the disturbance's center becomes displaced to the north, with the maximum in precipitation occurring slightly to the north of the maximum SST at the longitude of the disturbance. Compared to the mature phase, the decaying phase has a much more equatorially asymmetric structure, with a strong southwesterly flow at low levels accompanying the heaviest precipitation.

Figure 11 shows a vertical, north-south cross-section of this disturbance when it was located near $x = 16000$ km, a region with SSTs resembling those in the east Pacific. The updraft is quite broad in latitude in this case and is relatively intense. Low-level southwesterly winds feed the updraft. There is a strong southern hemisphere subtropical jet in this case.

In contrast, a suppressed period previous to the passage of this disturbance exhibits a very different circulation, as figure 12 shows. In this case the low-level winds are from the east and the updraft is much weaker than in figure 11. The upper-level subtropical jet is stronger and closer to the equator.

The time-mean circulation is shown in figure 13. Easterly winds predominate at the surface as in figure 12, and the vertical circulation is weak.

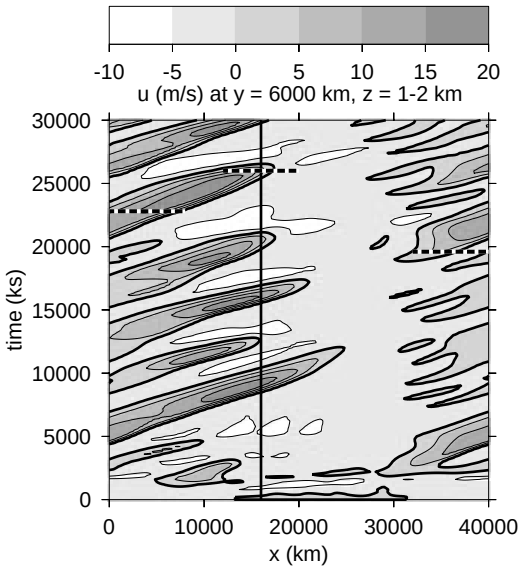

Figure 7: Latitude-time plot of zonal wind at $y = 6000$ km, averaged over the height range $1 - 2$ km. The dashed lines indicate sections displayed in figures 8, 9, and 10. The vertical solid line indicates the location of the "east Pacific" section.

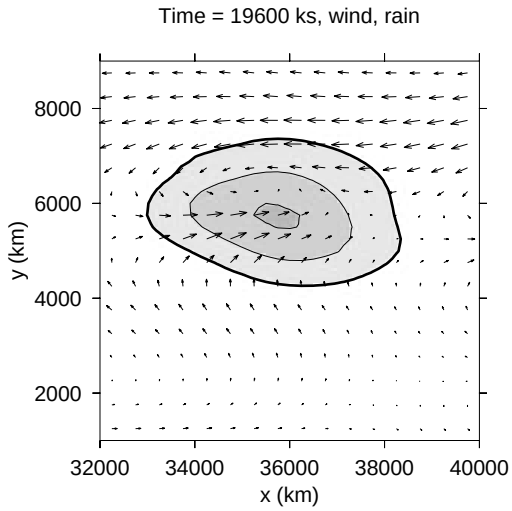

Figure 8: Snapshot of rainfall rates (contours and shading) and winds (arrows) at time 19600 ks averaged over elevations of $1 - 2$ km. The wind arrow scale is 10 m s^{-1} per 500 km and the rain contour interval is 4 mm day^{-1}, with the thick contour indicating a rate of 4 mm day^{-1}. The disturbance is intensifying in the "Indian Ocean".

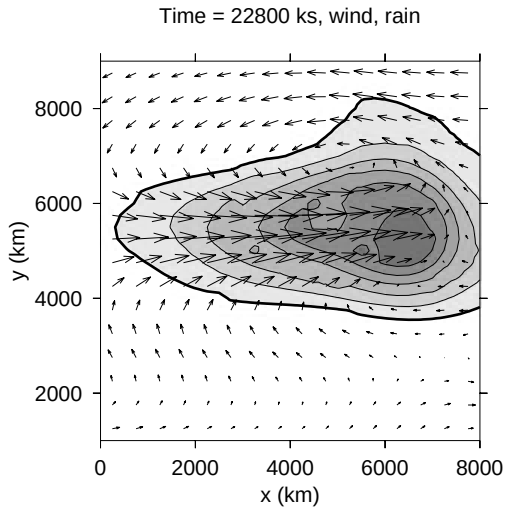

Figure 9: As in figure 8 except for time 22800 *ks. The mature disturbance is in the "western Pacific".*

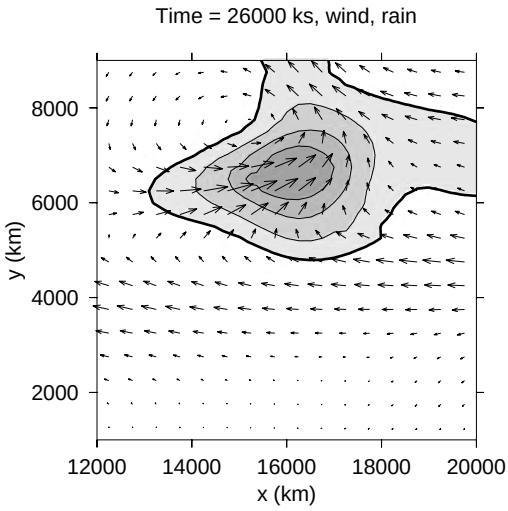

Figure 10: As in figure 8 except for time 26000 *ks. The decaying disturbance is in the "eastern Pacific".*

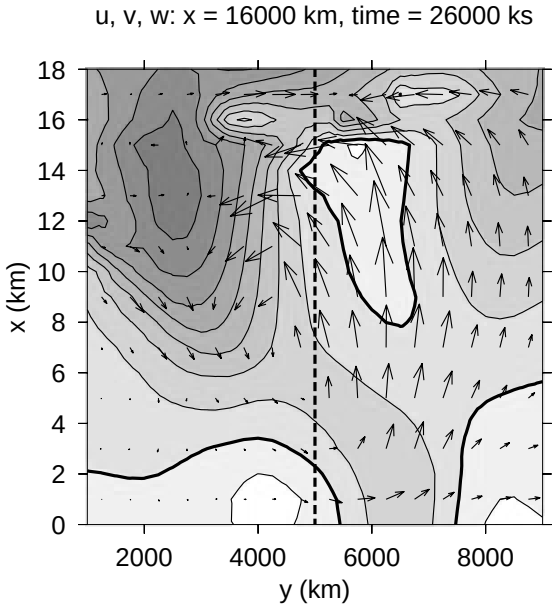

Figure 11: Zonal wind u (contours and shading) and flow in $y-z$ plane at $x = 16000$ km and time 26000 ks, i. e., during the strong convection phase of the MJO in the "eastern Pacific". The vertical dashed line represents the equator. The contour interval is 5 m s^{-1} with a heavy contour line indicating $u = 0$. Darker shades indicate stronger westerlies. The vector scale is 10 m s^{-1} per 500 km.

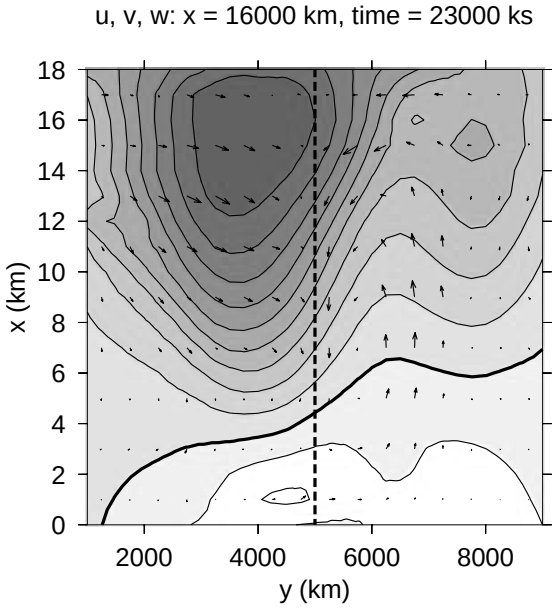

Figure 12: As in figure 11 except at 23000 ks.

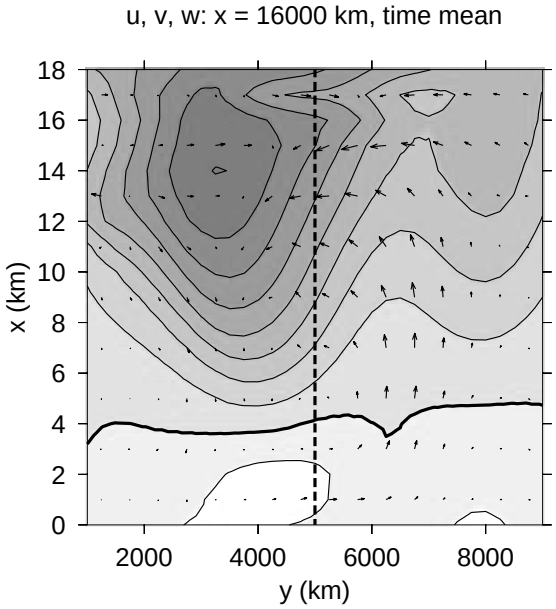

Figure 13: As in figure 11 except time-mean state.

4 Two-dimensional Hadley circulation

In this section the SST pattern at $x = 16000$ km, i. e., in the "eastern Pacific", is used to drive a two-dimensional, zonally symmetric circulation in the $y - z$ plane. Figure 14 shows the SST as a function of latitude in this simulation.

The time-mean circulation in the two-dimensional computation (which in this case is essentially steady after a period of spinup) is shown in figure 15. Comparison of this result with the time-mean circulation at $x = 16000$ km in the three-dimensional simulation illustrated in figure 13 reveals the existence of large differences between the two. In particular, the updraft in the two-dimensional simulation is stronger than in the three-dimensional case, but confined mostly to the equatorward side of the SST maximum. In contrast, the mean circulation in the three-dimensional case exhibits a maximum updraft well to the north of the SST maximum. In addition, the southern hemisphere subtropical jet is much stronger in three dimensions than in two.

5 Conclusions

The scale of variation of the SST in near-equatorial regions is typically much greater in the zonal direction than in the meridional direction. This leads to the expectation that the atmospheric flow which develops in response to this SST distribution should also be essentially two-dimensional, with approximate zonal symmetry.

The results of the present simulations, though employing a highly idealized approximation to the observed SST distribution and no land effects, strongly suggest that this expectation is not realized. In particular, the latitudinal extent and strength of the vertical atmospheric circulation in a region with cold water on and south of the equator (i. e., as in the east Pacific) is very different between the three-dimensional calculation and the two-dimensional approximation.

In addition, the two-dimensional calculation quickly leads to an essentially steady circulation, whereas the three-dimensional calculation is highly time dependent, as a result of the development of eastward-propagating MJO-like disturbances. In this respect the three-dimensional calculation represents observational results much more faithfully than does the two-dimensional calculation, as comparison with EPIC2001 results indicates.

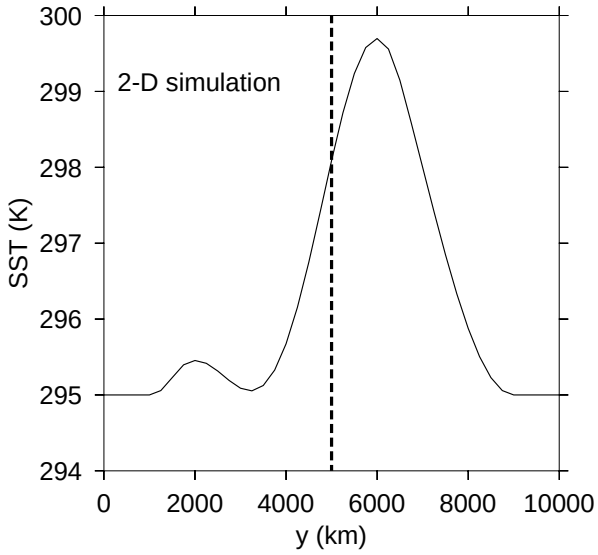

Figure 14: North-south cross-section at $x = 16000$ km of SST pattern shown in figure 6.

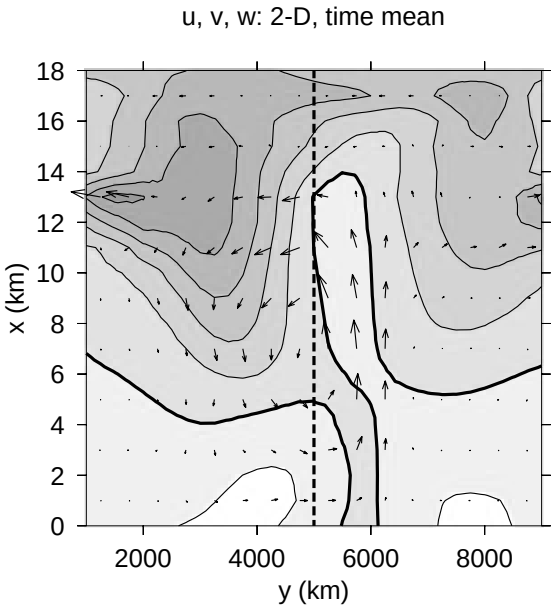

Figure 15: Time-mean, two-dimensional flow resulting from the SST pattern shown in figure 14. See figure 11 for plot details.

Acknowledgments. This work was supported by US National Science Foundation Grants ATM-0082612 and ATM-0079984.

6 References

Madden, R. A., and P. R. Julian, 1994: Observations of the 40-50 day tropical oscillation — a review. *Mon. Wea. Rev.,* **122,** 814-837.

Maloney, E. D., and D. L. Hartmann, 2000: Modulation of eastern north Pacific hurricanes by the Madden-Julian oscillation. *J. Climate,* **13,** 1451-1460.

Maloney, E. D., and D. L. Hartmann, 2001a: The Madden-Julian oscillation, barotropic dynamics, and north Pacific tropical cyclone formation. Part I: Observations. *J. Atmos. Sci.,* **58,** 2545-2558.

Maloney, E. D., and D. L. Hartmann, 2001b: The Madden-Julian oscillation, barotropic dynamics, and north Pacific tropical cyclone formation. Part II: Stochastic barotropic modeling. *J. Atmos. Sci.,* **58,** 2559-2570.

Molinari, J., and D. Vollaro, 2000: Planetary- and synoptic-scale influences on eastern Pacific tropical cyclogenesis. *Mon. Wea. Rev.,* **128,** 3296-3307.

Raymond, D. J., 1995: Regulation of moist convection over the west Pacific warm pool. *J. Atmos. Sci.,* **52,** 3945-3959.

Raymond, D. J., 2001: A new model of the Madden-Julian oscillation. *J. Atmos. Sci.,* **58,** 2807-2819.

Raymond, D. J., S. K. Esbensen, M. Gregg, C. S. Bretherton, L. K. Shay, C. Ohlmann, W. A. Peterson, 2003a: EPIC2001 and the coupled ocean-atmosphere system of the tropical east Pacific. *Bull. Am. Meteor. Soc.,* in revision.

Raymond, D. J., G. B. Raga, C. S. Bretherton, J. Molinari, Carlos López-Carillo, and Ž. Fuchs, 2003b: Convective forcing in the intertropical convergence zone of the east Pacific. *J. Atmos. Sci.,* 60, 2064-2082.